

# Field Experience with the Back-Pressured $K_0$ Stepped Blade

RICHARD L. HANDY, CHRIS MINGS, DAVID RETZ, AND DONALD EICHNER

The  $K_0$  stepped blade measures lateral pressures in situ in clay, silt, and sand soils. Pressures are measured after penetration of the soil by progressively thicker steps of a thin blade, and data points identified as representing consolidating behavior of the soil are extrapolated to obtain a hypothetical pressure on a zero-thickness blade. Pressures are measured with Teflon-covered pneumatic pressure cells designed to give 1-1 calibrations and ease of field repair. A new back-pressured readout system gives data reproducible to the nearest gauge dial increment, 1 psi (7 kPa). Most applications involve defining the soil stress history by measuring and plotting lateral stress versus depth. In nonexpansive soils the amount of prior surcharge may be estimated and the consolidation state established. Lateral stresses were used to delineate influences from compaction, expansive clays, adjacent shallow foundation loading, and interactions with pile and with retaining walls. For example, the lateral pressure on an existing wall was measured to test for pressures from expansive clay, relevant to the existing factor of safety. Passive pressures may indicate expansive clays or may warn of imminent bearing capacity failure per a cited example. Tests cannot be performed in stony soils, owing to difficulty in pushing the blade and the risk of damaging the pressure cells, nor can lateral stresses be measured in very soft clays where pressures from insertion of the blade exceed the limit pressure, which is probably attributable to the development of excess pore water pressure.

## PRINCIPLE

The  $K_0$  stepped blade was developed to measure lateral soil pressures in situ. The blade is rectangular, sharpened at the lower end, and becomes progressively thicker up the shank in a series of flat rectangular steps (Figure 1). Each step has its own pressure cell to measure the lateral soil pressure exerted on that step after the blade has been pushed into the soil. Tests are performed by drilling to above the test depth and then alternately pushing one step length and reading all embedded pressure cells. Thus, a series of pressure readings is obtained at each subdepth. By plotting the several step pressures measured at each subdepth as a function of the step thickness, an extrapolation may be made (as indicated in Figure 1) to give hypothetical pressures on a zero thickness blade as an indication of the lateral total stress existing in the soil before blade insertion. Effective stresses are estimated by subtracting static pore pressures calculated from depth below a water table or measured with piezometers.

R. L. Handy and D. Eichner, Department of Civil and Construction Engineering, Iowa State University, Ames, Iowa, 50011. C. Mings, Geo-Hydro Engineers, Inc., 100 E. Callahan St., Rome, Ga., 30161. D. Retz, Burns & McDonald Engineering, 4600 E. 63d St., Kansas City, Mo. 64141.

## HISTORY

The stepped blade was developed for the U.S. Federal Highway Administration to provide a rapid and accurate alternative for measuring lateral in situ stress in soil. The goal was a method that would be accurate to within 1 lb/in.<sup>2</sup> (7 kPa) and be more rapidly and more readily performed than self-boring pressuremeter tests. The approach described here was borrowed from analytical chemistry; that is, to recognize that some disturbance to the soil is inevitable if a hole is bored or an instrument inserted into the soil so that instead of attempting to prevent disturbance the disturbance is allowed to happen and its effects removed by extrapolation.

The initial development of the stepped blade was made by Soil Systems, Inc., Marietta, Georgia, with Iowa State University as subcontractor from 1976 to 1981 under FHWA sponsorship. Tests and developments were continued at Iowa State from 1982 to 1987, with Eichner Engineering Co. as subcontractor for developmental work and J.-L. Briaud's group at Texas A&M University doing the comparative pressuremeter and finite-element studies. During this time the blade went through five major redesigns, the latest incorporating a back-pressure readout system and a back rib to stiffen and strengthen the blade without appreciably affecting pressure readings.

The blade development was preceded and was partly inspired by the pioneering work of Marchetti with the dilatometer. The main differences between the stepped blade and the dilatometer follow: The blade has several steps, each with its own pressure cell, and is several times thinner than the dilatometer. The blade cells are pneumatic and nonexpansive, and the dilatometer is electropneumatic and expansive. The dilatometer is shorter and more rugged and can be pushed continuously, and the blade requires predrilling to each test depth where it then is pushed. The soil responses differ, as do the methods for data interpretation. The dilatometer interpretations depend more on established empirical correlations.

## DEVICE

### Ratio of Width to Thickness

Most in situ soil testing devices are cylindrical in shape, with the lower end sharpened to a cone or hollow cone. An obvious difference between pushing a thin, flat blade and pushing or driving a cone is the reduction of the amount of soil displaced and disturbed. Further, the thinner the blade, the less soil should be disturbed.

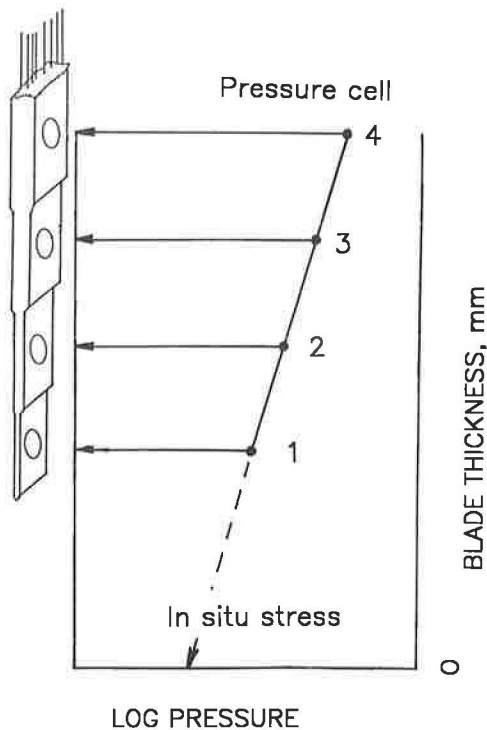


FIGURE 1 Principle of the  $K_0$  stepped blade test.

Laboratory tests with layered modeling clay showed a linear relationship between the thickness of the disturbed zone and the thickness of the blades, the blade width being constant ( $l$ ). The ratio of width to thickness can be used as a dimensionless measure of relative blade thinness: the higher the ratio, the thinner the blade. In the case of solid cylindrical or conical test devices, the ratio is 1.0. Ratios for those and other devices including the current stepped blade are listed in Table 1 and presented in Figure 2. In the case of the two samplers listed, the ( $w$ ) is taken as the inside circumference of the sampler and the thickness ( $t$ ) is twice the wall thickness, since soil is displaced only toward the outside.

**Back-Pressured Pneumatic Pressure Cells**

A late development in blade research, and a key factor for improving the reliability and precision of the pressure readings, was the invention of a back-pressured system for operating and reading the pneumatic pressure cells (2). Most pneumatic cells, including those of earlier model blades, operate by applying inside gas pressure against a diaphragm exposed to the pressure to be measured. Then, when the pressures are equalized, the diaphragm lifts sufficiently to allow gas to flow through the cell and be detected with a flowmeter. Those are referred to as normally closed or venting type cells (3). In early versions of the blade, pressure was applied to area A in Figure 3, and area B was monitored for flow. After flow had been achieved, gas pressures may have been reduced to obtain a pressure reading for the initiation of a no-flow condition. This was not done in early blade testing because of the undesired effect of pushing the soil away and then allowing

TABLE 1 WIDTH-THICKNESS RATIOS FOR SOME SOIL PENETRATION TEST AND SAMPLING DEVICES

Device	t, mm	w, mm	w/t
Standard cone	35.7	35.7	1.0
SPT	15.9	110	6.9*
3-in. Shelby tube	3.3	229	69.4*
NX vane	3.2	25.4	8.0
Dilatometer	14	95	6.8
Glötzl cell	5	100	20.0
SBT step 1	3	63.5	21.2
step 2	4.5	63.5	14.1
step 3	6	63.5	10.6
step 4	7.5	63.5	8.5

\* t is 2X the wall thickness and w is the inside circumference since the soil is presumed to be displaced only to the outside.

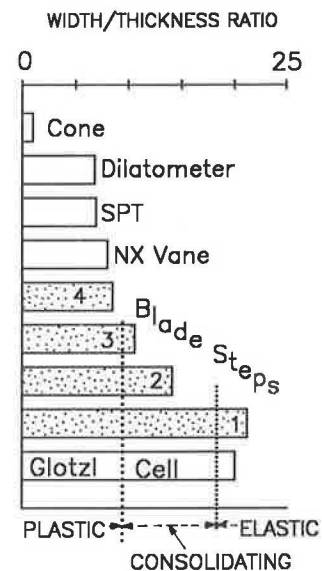
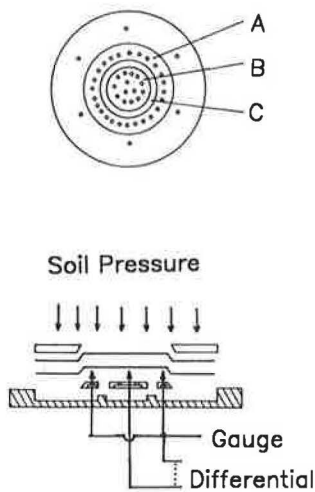


FIGURE 2 Width/thickness ratios for some soil-penetrating devices and dominating behavior as inferred from stepped blade tests.

the soil to come back before taking a pressure reading. Difficulties were experienced when the diaphragms either leaked or stuck when monitoring for changes in gas flow through long pressure lines. In some instances, individual blade cells had calibration factors that not only were different for each cell but tended to change (4). A strain-gauge cell that directly measures effective stress also was developed (5) but was not sufficiently reliable for field use, so emphasis continued to be placed on the pneumatic cell.



**FIGURE 3** Components of the pneumatic pressure cell (not to scale).

Laboratory tests indicated that sticking of diaphragms was more likely to occur at high pressures and be quite sensitive to minor changes in the height of the threshold C in Figure 3. Because only part of the back side of the diaphragm was pressurized, which seemed a rather inefficient and possibly error-prone way to balance the soil pressure, a scheme was devised to pressurize both areas A and B simultaneously while maintaining a small differential pressure between the two areas. When the higher of the two pressures reached the soil pressure as the two pressures were raised, the membrane lifted sufficiently to allow a small amount of gas flow within the cell, thereby reducing the differential pressure to near zero and usually causing a perceptible pause in the rate of increase of the main gauge pressure. The loss of differential pressure told the technician when to read the pressure gauge, and the serendipitous pause in climb of the main gauge needle made it easier to read.

The method used for simultaneous pressurization is quite simple and is presented schematically in Figure 4. A needle valve T1 controls the rate of pressure increase and ordinarily is set for a rate of increase of about 1 psi/s (7 kPa/s). Nitrogen, compressed air, or carbon dioxide regulated to a maximum pressure of 300 psi (2000 kPa) is used as a gas source. The second needle valve T2 is left closed until both gauges approach 8 to 10 psi (60 to 80 kPa), and then the needle valve is opened slightly and adjusted to give a differential pressure that will tend to remain constant without further adjustment. Some leakage and reduction of differential pressure may occur as the soil pressure is approached, particularly if the soil pressure is unevenly distributed around the cell threshold C in Figure 3. In this case, T2 may be partially shut to sustain  $\Delta P$  until a sharp drop occurs. It will be seen that if the diaphragm is lifted, then  $\Delta P$  must go to near zero regardless of the position of T2.

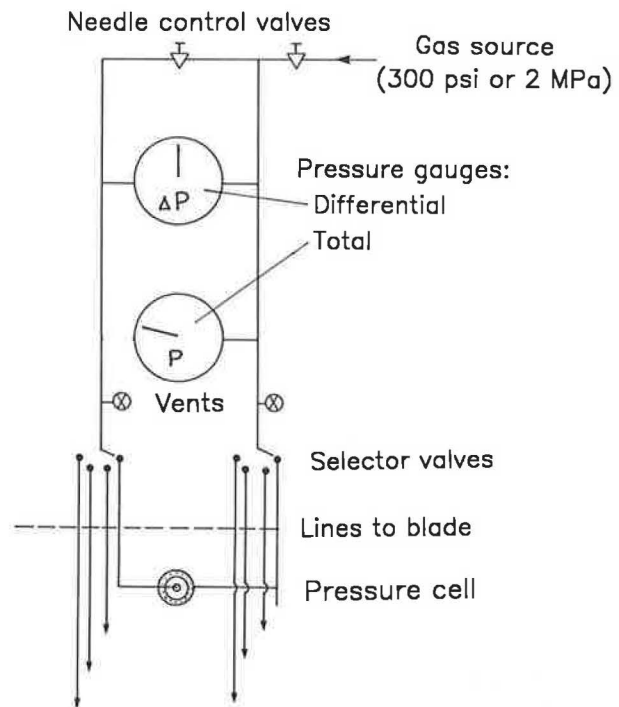


**FIGURE 4** Schematic diagram of the back-pressured blade console.

## SOIL RESPONSES

### Consolidation Response

It was anticipated and then shown by laboratory experiments that the thicker the blade step the higher the pressure induced by insertion of that step into the soil ( $I$ ). An empirical relationship was defined between thickness and log pressure, as indicated in Figure 5a. Regression of the data typically will give  $r^2$  values in the range 0.97–1.0. The semilogarithmic response corresponds to a linear relation of void ratio to log pressure and on this basis is assumed to be indicative of consolidating behavior of the soil next to the blade. Consolidation may be aided by the relative thinness of the blade when compared with other devices and by a zone of reduced stress and low or negative pore pressures extending out from both edges of the blade after insertion. Because consolidation may be far from complete when blade cell pressures are read, approximately the same amount of time should lapse between insertion and reading of each pressure cell. Variable times from a few minutes to 2 weeks have been used without affecting the extrapolated soil pressures.

### Elastic Response

Field use of the stepped blade indicated that the soil response might not always be so simple as was initially envisioned. The pressure sometimes is higher on the first and thinnest blade step than on the subsequent thicker steps. This behavior, presented in Figure 5b is followed by the more conventional behavior.

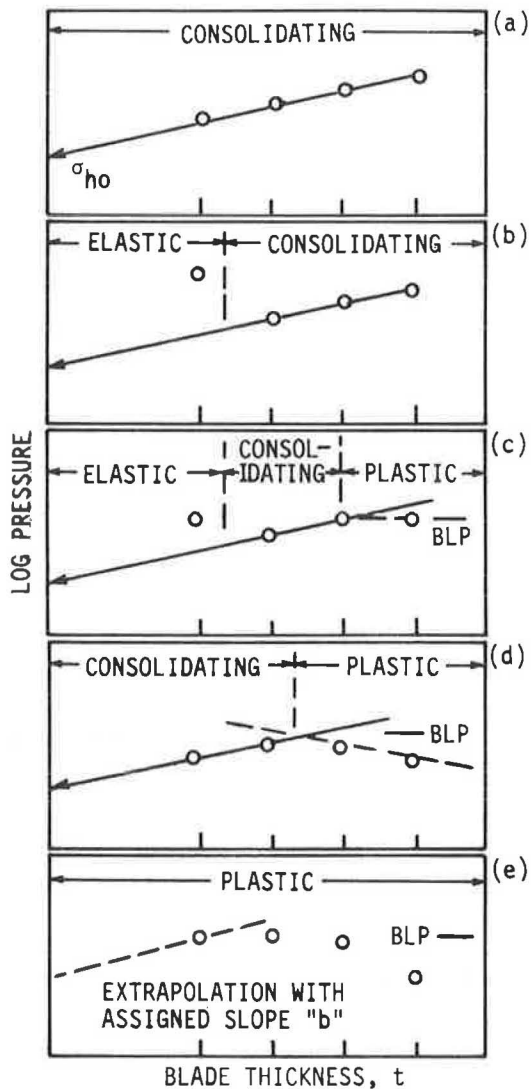


FIGURE 5 Selected data plots of log blade pressure as a function of blade thickness  $t$  and inferred soil response. BLP, blade limit pressure.

This anomaly did not occur in the laboratory developmental tests performed on remolded samples (1) and was most commonly observed in stiff clay loam soils such as glacial till and in lightly cemented silts and sands. Circumstantial evidence thus pointed to influences from a relict soil structure that may be left intact by penetration of the thinnest blade step only. The structure may cause the soil to behave elastically until broken down by penetration by the next thicker step.

The blade imposes constant deflection instead of constant stress conditions, as in a conventional laboratory consolidation test. Thus, as illustrated in Figure 6, a stress relief from B on the elastic response curve to C and D on the virgin compression curve should be possible if the soil structure were to break down. An analogous reduction does not occur in constant-stress consolidation tests because the path goes from C downward to E. When it occurs, this apparent discontinuity in soil behavior indicates that data should be separated into two stress regimes.

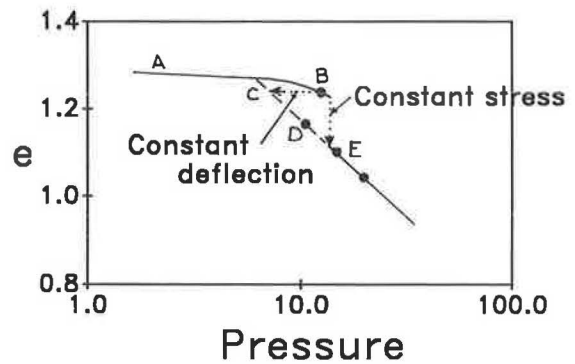


FIGURE 6 Hypothetical  $e$ -log  $p$  diagram of a slightly cemented soil to show how a high first point may develop in stepped blade tests. Collapse of the soil structure relieves the stress from B to C and D on the virgin compression curve.

If this interpretation is correct, then the pressure on the first step should be essentially an elastic response that may be used to compute a lateral subgrade modulus. In support of this, correlations between first-step pressures and the pressuremeter moduli were substantially better than were obtained by subtracting consecutive step pressures (6).

In no case was the elastic response observed on other than the first blade step, indicating that a width/thickness ( $w/t$ ) ratio that is less than 14 must break down the soil structure. A value of 18 was arbitrarily selected to define an approximate elastic range indicated in Figure 2.

#### Plastic Failure

A second, more common, departure from a semilogarithmic relationship between soil pressure and blade thickness was previously described and attributed to a limit pressure; that is, relief of the consolidating pressure by plastic failure where the dominating behavior is pushed aside rather than being compressed (1). This behavior is noticed when there is a constant or decreasing blade pressure with increasing step thickness, as indicated on the right in Figures 5c, 5d, and 5e. The phenomenon is most common in soft, saturated clay soils where it probably reflects the development of excess pore pressure. What supports this interpretation is that the blade limit pressure has been shown to correlate with the pressuremeter limit pressure (6), and soil pressures measured in soft clays with the relatively thick dilatometer have been shown to be mainly excess pore water pressures (Lutenegger, unpublished data). A pore pressure port has been incorporated into the thickest step of the blade but has not yet been subjected to field tests. Pore pressure studies to illustrate consolidating behavior with the thinner blade steps are reported by Tse and Handy (7). The limit pressure response usually occurs by the fourth step and in soft soils may also occur when inserting thinner steps and, in some instances (as indicated in Figure 5e), preventing a meaningful extrapolation in obtaining a lateral in situ stress.

Because plastic failure often occurs with insertion of the fourth blade step, the consolidating response mechanism appears normally to be limited to  $w/t$  ratios that are less than

8.5, which is the value indicated in Figure 2. However, plastic failure is not inevitable with the fourth step, and the limiting  $w/t$  ratios will vary with the individual soil and moisture condition.

**Implications**

Although at first considered a nuisance, the different modes of soil behavior suggested in this analysis can give additional information relative to the tested soil and also may give important insights into other in situ test methods. For example, it would appear from Figure 2 that the pushing of cones—whether Dutch, piezo, expandable, or ice cream—can be expected to cause plastic failure sufficient to modify previously existing lateral stresses and to bring those stresses to a limit pressure. On the basis of their  $w/t$  ratios, the same interpretation may be applied to the stepped blade and dilatometer. This can be advantageous by removing the influence of variable  $K_o$  and by allowing a focus on other material properties. Where the stepped blade and dilatometer have been used in the same soil,  $P_o$  pressures measured with the dilatometer are approximately the same as pressures measured by the thickest section of the stepped blade, both having about the same  $w/t$  ratios and appearing to induce limit-pressure responses. This also means that sleeve friction on a cylindrical probe probably is not a valid measure of both lateral stress and  $K_o$ , which existed before insertion of the test device, but be more a function of the limit pressure. The elastic modulus obtained with the dilatometer derives from the pressure to bulge out its central diaphragm, which probably does not reinitiate plastic failure. However, this also implies that the modulus measured by the dilatometer is buffered by an intermediate zone that has undergone plastic failure, supporting the need for empirical correlations.

Also, Figure 2 indicates that the only devices that appear to be thin enough to be pushed into soil without inevitably collapsing its structure are the Glotzl cell and the first step of the stepped blade. A correlation was discovered by Lutenecker (unpublished data) between the maximum elastic response pressure that can be measured by the blade and the lateral preconsolidation pressure as influenced by, for example, cementation or aging stress history. This is reasonable because pressures in excess of this amount should break down the soil structure and cause the soil to enter a consolidating stage.

The blade appears unique among in situ test instruments in showing an identifiable consolidating behavior. For example, the pressuremeter expanding in a prebored hole may be interpreted as causing elastic response with direct transition into plastic shear and perhaps be related to the relatively poor drainage in this test.

It is important in the interpretation of blade data to recognize possible changes in response mechanisms to avoid error from collective consideration of dissimilar data (i.e., the “apples and oranges” effect). For example, data points that are low because of the attainment of a limit pressure will tilt the slope of the graph and give too high an extrapolated in situ stress.

A flow path designed to remove subjectivity in assigning and interpreting blade data is presented next.

Flow chart for interpreting stepped blade pressure readings:

1. First data point higher than second? Then, elastic response; do not include in extrapolation.
2. Last data points equal or lower than previous points, or plot low on the graph? Then, limit pressure; do not include in extrapolation.
3.  $r^2 < 0.97$  (where applicable). Then, reexamine data for influence from possible limit pressure.
4. Line slope  $< 0.05 \text{ mm}^{-1}$ , possibly negative? Then, all data probably exceed limit pressure; extrapolation not reliable.
5. Three or four points with  $r^2 > 0.98$  and with line slope  $> 0.05 \text{ mm}^{-1}$ ? Then, good test.

**Representative Data**

Representative data plots from tests in a hydraulic fill sand near San Francisco and a loessial silt in western Nebraska are presented in Figure 7. Test data from a soft alluvial clay in Nebraska, a medium stiff clay in Houston, and a very stiff clay near College Station, Texas, are presented in Figure 8. To reduce subjectivity in selecting the data to be shown, all are for tests at approximately the same depth, which was arbitrarily selected to be 15 ft (5 m). Only the uppermost,

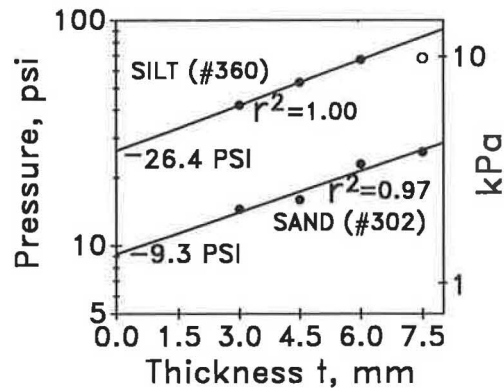


FIGURE 7 Representative test data for an unsaturated loessial silt and for a saturated sand. Open point was not included in the regression. Test numbers refer to Handy et al. (6).

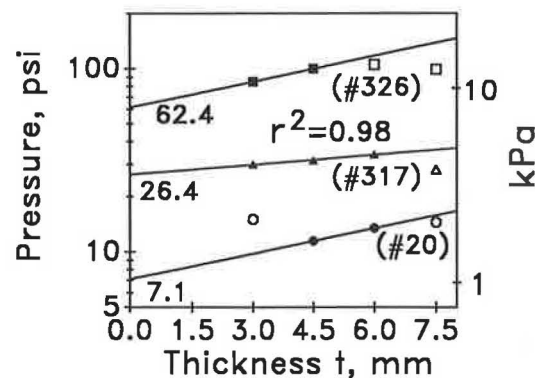


FIGURE 8 Representative test data for some clays. Open points were not included in the regressions, representing either initial elastic response or limit pressure.

four-point data sets are shown. (Additionally a three-point, a two-point, and a one-point set is obtained at each testing subdepth and is subjected to the same methods for data interpretation. Because of rapid variations in lateral stress with depth, probably as a result of localized influences and stratification, the data usually are not pooled or averaged but are reported separately.)

In Figure 7, the data plot for the silt indicates no elastic response and a high  $r^2$ , which supports the thesis that consolidation occurs and is the main factor that affects the measured pressures. A limit pressure was reached on the fourth blade step. The soil was not saturated, and  $K_o$  was calculated to be about 1.5, indicative of overconsolidation. Because the loess at this site has no known history of preloading but does contain montmorillonite, one interpretation is that the higher lateral stresses are attributable to aeolian deposition and drying followed by clay expansion on burial and wetting.

Also in Figure 7, the data for the sand show no clear indication of an elastic response or of a limit pressure and give an acceptably high  $r^2$ . The calculated value for  $K_o$  is about 0.8. As will be shown later, a graph of lateral stress versus depth in this sand indicates a small and measurable amount of overconsolidation.

In Figure 8, the very stiff clay is a Vertisol, meaning that field evidence indicates it has expanded to the point of lateral pressure relief through shearing (i.e., the passive earth pressure condition). Stepped blade measurements indicate that the lateral stress is quite high, giving  $K_o$  at the test depth of about 4. The limit pressure also is high, several times higher than the unconfined compressive strength, as would be expected for a lateral-bearing capacity-type failure.

The medium clay in Figure 8 also is a Vertisol, and blade tests at shallow depths at this site exactly duplicated lateral stresses obtained at the same site 6 years earlier with an older model blade (1)(6). At this depth,  $K_o$  is about 1.6. As is in the case of the very stiff clay, the limit pressure is several times higher than the undrained shear strength reported by Mahar and O'Neill (8).

The soft clay test in Figure 8 shows a breakdown of structure after penetration by the first step, suggesting that the pressure on that step may be used for calculation of a lateral subgrade modulus. The lateral stress is low for a soft clay, giving a  $K_o$  of about 0.5, which is possibly indicative of underconsolidation. This interpretation is consistent with the origin of this clay by recent sedimentation in an oxbow lake. The limit pressure approximates the calculated maximum for passive failure, which will be discussed later.

Those examples are included to show representative test data and soil responses. For full interpretations of stress history of a soil, it is necessary to determine the relationships between lateral stress and depth, which is the subject of the remainder of this paper.

## ILLUSTRATIONS OF USES OF THE $K_o$ STEPPED BLADE

### Determination of the Consolidation State

#### Overconsolidation

The stiff clays of Figure 8 are determined to be overconsolidated, indicated by  $K_o > 1$ , and be attributable to their

expansive nature. The shaded area in Figure 9 labeled "before pile driving" encloses a relatively narrow range of lateral stresses measured in this 50-year-old hydraulic fill sand. (The solid dot is the pressure extrapolated from sand data in Figure 7.) A trend line through the data intersects the ground surface at a lateral pressure of about 3 psi (21 kPa). The corresponding vertical surcharge load may be obtained by extending the trend line upward to intersect the y axis, which occurs at an above-ground height of 10.9 ft (3.3 m), indicating prior existence of that amount of surcharge or its weight equivalent. The prior surcharge thus obtained is 0.66 Tsf, indicative of a moderate degree of overconsolidation not unreasonable for a heavy-equipment storage yard. The slope of the trend line also allows an estimation of the friction angle from the Jaky equation. But, because this estimate is based on lateral stresses developed as a consequence of consolidation, it probably contains no dilatant component. The angle is 20 degrees, which is considerably lower than the total-strength friction angle estimated at this site from cone and stepped blade tests (6). The sand is micaceous, which also will contribute to low sliding friction.

### Normal and Underconsolidation

Figure 10 presents SBT data from the site of Jackson Lake Dam, Jackson Hole, Wyoming, after the dam had been removed because of a potential risk of liquefaction in this active earthquake area. The short-dashed line shows lateral stresses, calculated assuming  $K_o = 0.5$ , without the dam in place. Below

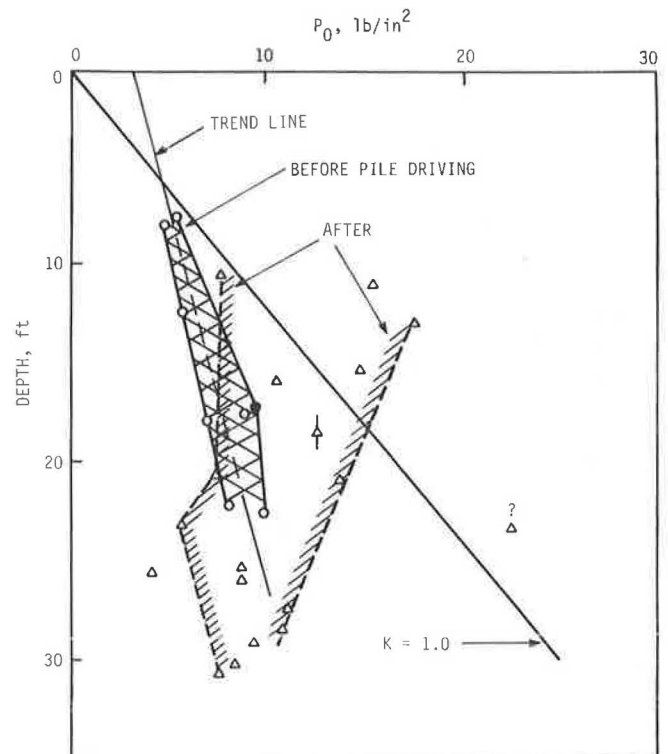
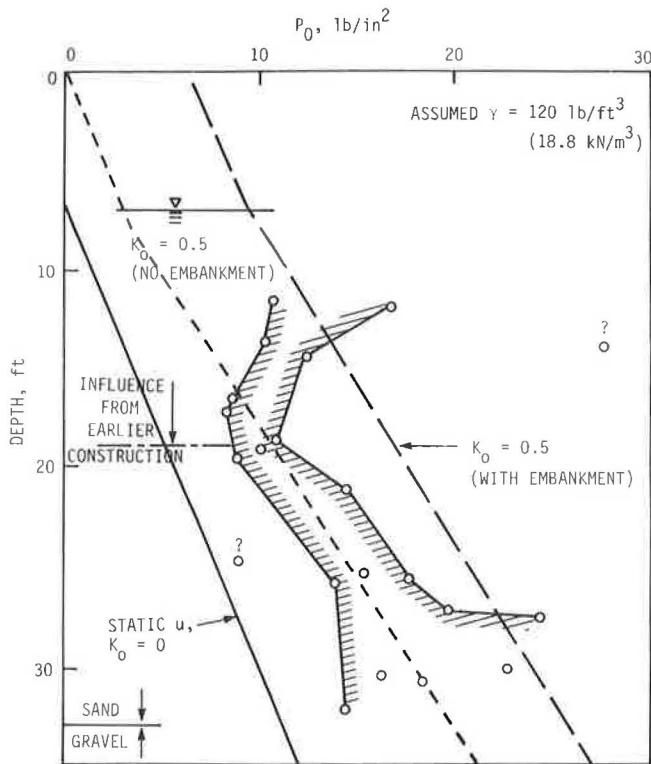


FIGURE 9 Lateral stresses measured in a sand at Hunter's Point Naval Base, San Francisco. Note that  $K$  lines are calculated based on effective stress and then are converted to total stress as measured by the blade.



**FIGURE 10** Lateral stresses in sands and silts at Jackson Lake Dam, Wyoming, after removal of the dam and before dynamic compaction.

a depth of about 19 ft (6 m) the line approximately bisects the data, which indicates that the soil there is normally consolidated if no consideration is given to the weight of the dam. With the dam in place, soil below this depth will be under-consolidated, which supports the thesis that the dam indeed is threatened by potential liquefaction of foundation soils, at least in the depth zone from 19 to 33 ft. At shallower depths the lateral stress data trend upward, approaching the  $K_o = 0.5$  line. It, therefore, may be concluded that at the shallower depths the soil is normally consolidated under the weight of the dam, probably caused by the greater concentration of surcharge load at those depths. Many other devices, including the Menard pressuremeter, self-boring pressuremeter, and dilatometer, also were used at this site, with the dilatometer giving the most closely comparable lateral stress results (12).

Those examples illustrate the use of lateral stress data to diagnose the soil consolidation state without the necessity for sampling and laboratory determination of a preconsolidation pressure, which is very sensitive to sample disturbance and is all but impossible to determine from laboratory tests of a sand. Such information can be vital. For example, tests recently were performed for a metro tunneling project underneath an interstate highway, and the tests gave an unexpected result: the silt soil, presumed to be residual and hence under high lateral stress from weathering expansion, actually was normally consolidated, thus signaling that any additional load would cause appreciable settlement. On the other hand, in overconsolidated nonexpansive soils, the inferred prior load should indicate how much load can be added without exceeding the preconsolidation pressure and causing appreciable settlement.

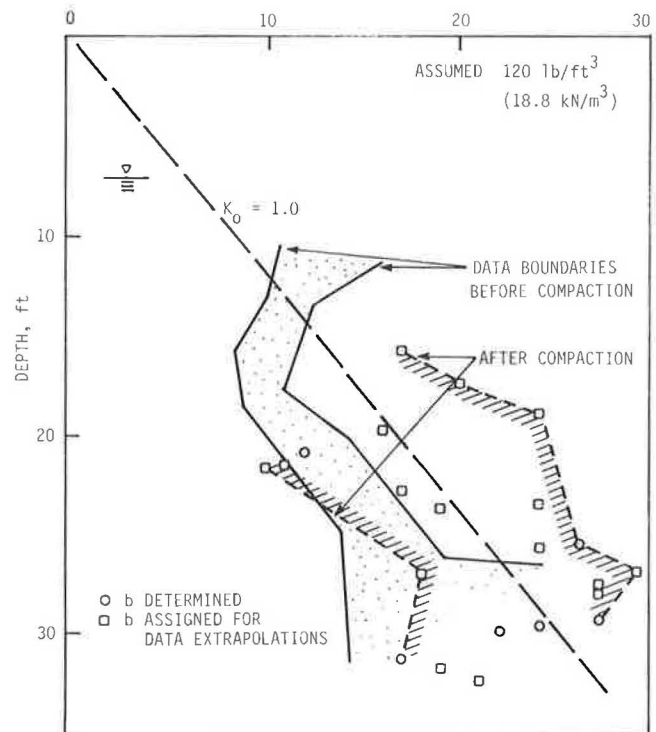
*Detection of Artificial Compaction*

Figure 11 presents lateral stresses measured at the Jackson Dam site after dynamic compaction. Because the data are so erratic, an interpretation technique was used that involved determining average slopes “b” from the data plots and then applying that slope to individual points (I). While this did not reduce the data scatter—in fact it increased it—the additional points allow a range of lateral stresses to be sufficiently well defined to suggest that the average  $K_o$  after compaction is about 1.0, which indicate liquefaction during compaction and represent a substantial increase over the previous value of 0.5. The lateral stresses also are in the proper range for normal consolidation with the dam replaced, indicating that the soil now may be safe from liquefaction.

Figure 12 presents data obtained in back-fill soil behind a bridge abutment. Most of the lateral stresses are far below the line for  $K_o = 1$ , indicating that the soil had not been compacted. However, scattered high points, up to about 8 psi (60 kPa), occur scattered throughout the height of the embankment. Those random high stresses have the correct magnitude to have been caused from wheel contact pressures from earth-moving equipment during construction of the embankment.

*Detection of Grouting*

While rather incidental to the studies at hand, one of the abutments in Figure 12 give some perplexingly high lateral stresses in the upper 11 ft (3.4 m) of soil, as high as 24 psi (165 kPa), plotting far off of the graph to the right. It later was discovered that this soil had been pressure grouted to



**FIGURE 11** Test results from the Jackson Lake site of Figure 10 after deep dynamic compaction.

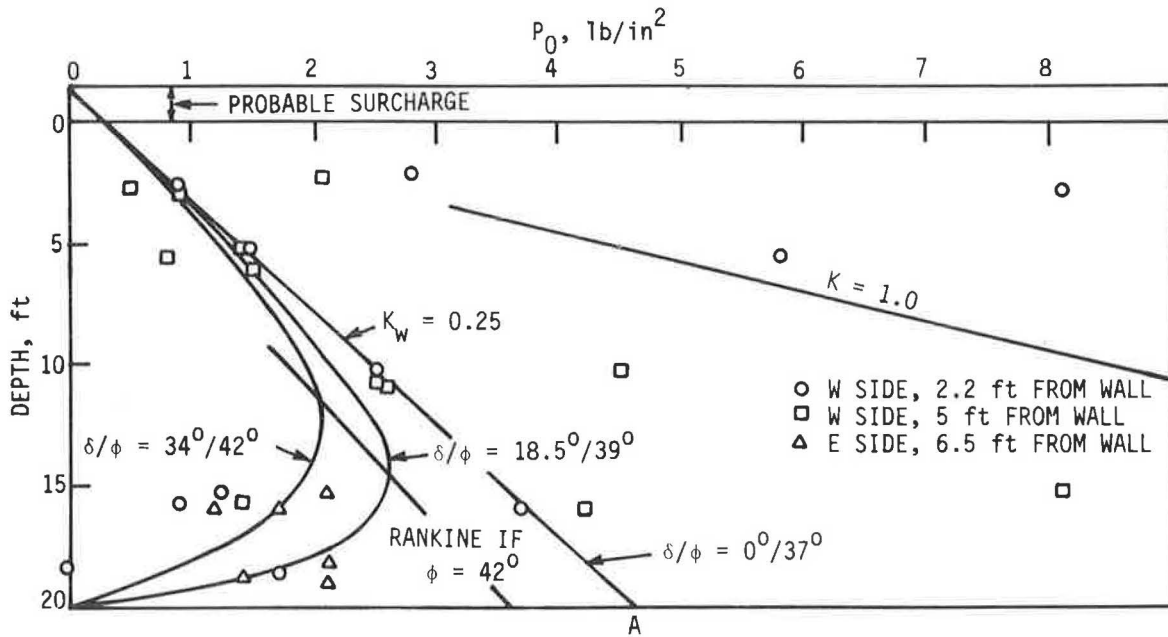


FIGURE 12 Pressures against bridge abutments compared with predictions from Rankine and from a recent arching theory (10). Data courtesy of Clyde Anderson, CTL/Thompson, Inc., Kellogg Engineering, Inc., and the City of Lakewood, Colo.

raise the approach slab. The average  $K_o$  in this zone is about 3, so pressures should have been high enough to do the job.

Passive Pressures

Bearing Capacity Failure

Figure 13 presents the distribution of lateral stress with depth in a soft oxbow lake clay immediately adjacent to a highway embankment then under construction. The tests were con-

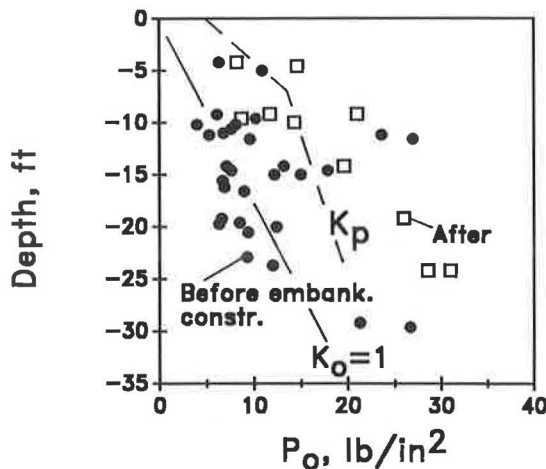


FIGURE 13 Lateral stresses in a soft lake bed clay adjacent to a highway embankment, Storz Expressway, Omaha, Nebr. Solid points are before embankment construction and open squares after, when there was concern for an impending bearing capacity failure.  $K_p$  line was drawn based on preconstruction shear tests.

ducted before construction began and later when settlements became excessive and slope indicators showed lateral bulging outward of the foundation soil (13). Lateral stresses are approximately twice what had been measured prior to the construction and exceed the theoretical maximum dictated by  $K_p$  calculated from borehole shear test data. Those data were obtained before construction and do not reflect a probable increase in strength from the partial consolidation. The excessive settlement of the embankment, lateral bulging of the foundation soil, large increase in lateral pressures, and their proximity to  $K_p$  pressures suggest that it would be judicious to adjust the construction schedule to allow further dissipation of excess pore pressures through previously installed wick drains. This was done. The embankment was completed the following construction season without incident.

Expansive clay

Tests presented in Figure 12 were performed in soil that was known to be expansive to determine if it was exerting undue pressure on adjacent bridge abutments. As can be seen from the data, this turned out not to be the case, because generally  $K_o \ll 1$ . The bridge was removed without difficulty.

Figure 14 presents lateral pressures versus depth in the very stiff expansive clay, including the data point from Figure 8. The shaded zone includes three-fourths of the data points in a relatively narrow band. Because  $K_o \gg 1$  and because this is a known Vertisol, passive conditions are suspected. To test this premise, two points were selected on the linear trend line for substitution of lateral and vertical stresses into the passive pressure equation. Then it was solved simultaneously to give drained shear strength parameters. The equation is

$$\sigma_h = \gamma z \tan^2[45 + (\phi/2)] + c \tan[45 + (\phi/2)] \quad (1)$$

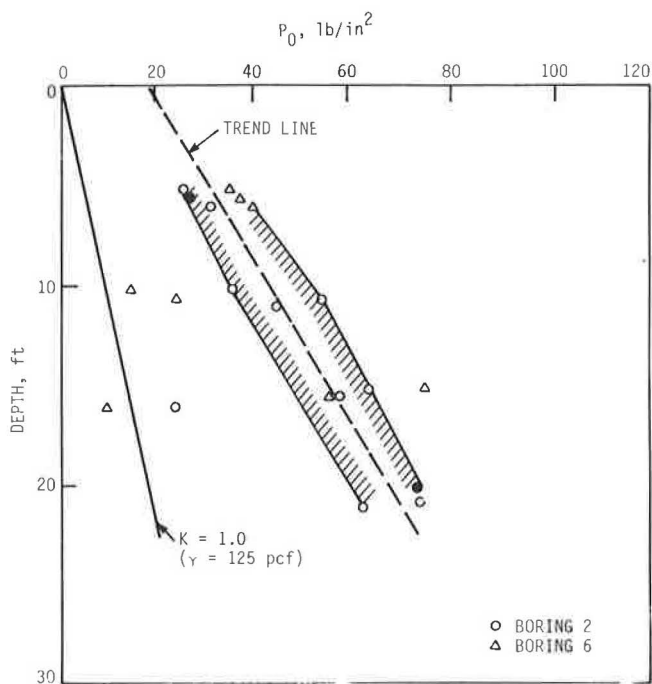


**FIGURE 14** Lateral stress data from a very stiff expansive clay. Data from Texas A&M University, College Station, Texas.

By using this procedure with the data from Figure 14, one obtains  $\phi = 28$  degrees and  $c = 11.3$  psi (78 kPa). The equivalent unconfined compressive strength calculated from those values is 19 psi or 1.4 Tsf (131 kPa), which compares favorably with measured values that ranged from 0.8 to 1.6 Tsf, averaging about 1.2 Tsf (6) (9). This would appear to confirm that lateral stresses in this soil are being limited by passive failure and also demonstrates how lateral stress data versus depth multiplied by soil unit weight can be used to approximate drained  $c$  and for  $\phi$  if the soil is in the passive state.

### Slope Stability

Unfortunately, the potential for the blade test to measure passive pressures at the base of slopes and thus detect the potential for slope failure before movement occurs has not yet been realized owing to the difficulty of getting drilling machines into landslide toeslope areas. This application would appear to be useful for preventative maintenance of cut and fill slopes, because it should be cheaper and more effective to repair a slope before failure occurs than after the soil has moved and become permanently weakened through remolding and from dilatant shear creating suction and increasing water contents in the shear zone. Figure 15 indicates where pressures might appropriately be measured on the basis of finite-element analyses (11). As simulated excavation proceeds, progressive failure and the potential development of passive pressures should initiate in soil in the toe zone even though the overall factor of safety still exceeds 1.8. The detection of high lateral stresses in a toeslope thus would flag when preventative measures should be undertaken or when stability

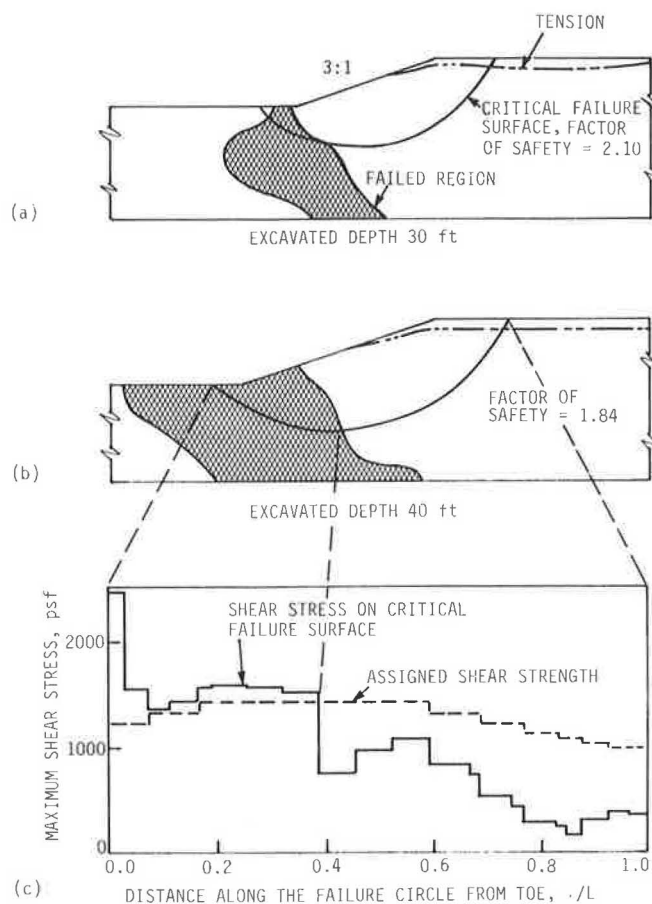


**FIGURE 15** Hypothetical failure zones from finite-element analyses of a 3-1 slope excavated in overconsolidated clay. Data from Dunlop and Duncan (10).

of the slope should be reevaluated by a method of slices with soil strengths reduced for toe slices by a factor equal to the soil sensitivity.

Low lateral in situ stresses have been measured in soil above an active landslide in the zone frequently marked by the development of tension cracks.

### Pressures Adjacent to Existing Structures and Driven Pile

Figure 12 presents lateral pressures measured in soil close to an existing wall, as has already been discussed. Figure 9 presents the increase in shallow lateral soil stresses as the result of driving pile and the erratic disposition of lateral soil pressures near the pile tip. The latter may help explain why test loading indicated that the pile group action factor at this site is about 1.

### Subgrade Modulus and Limit Pressure

An estimate for a lateral subgrade modulus  $k_b$  is obtained by dividing the pressure measured on the first blade step by one-half the blade thickness, or 1.5 mm. The value of the modulus

depends in part on the size of the area being loaded, and experience with those  $k$  values is very limited and is not in the scope of this paper. Application of elastic theory to a blade area considered as a surface load gives the following relationship between  $k$  and the elastic modulus  $E$ :

$$E = 2.8 k \quad (2)$$

Application of this equation to the Houston clay data gives  $E$  values comparable to those obtained from UU triaxial tests and lower by an order of magnitude than those obtained from cross-hole seismic studies (8). The modulus thus obtained from blade tests in a sand appeared to give an accurate prediction of settlement of a bridge abutment (6).

## CONCLUSIONS

1. Elastic, consolidating, and limit pressure modes of soil behavior are suggested by different lateral pressure responses to penetration by different thickness steps of the  $K_o$  stepped blade. The consolidating mode is used for extrapolation to obtain hypothetical in situ pressure on a zero thickness blade.

2. The pattern of lateral in situ stresses with depth in sand, silt, and clay soils can be used to define the soil consolidation state and, in nonexpansive soils, to indicate the amount of prior surcharge or overburden. Lateral stresses usually are higher than from normal consolidation and are attributable to geological or man-induced unloading, clay expansion cycling, and, in residual soils, expansion of minerals on hydration weathering.

3. Lateral in situ stresses show influences from mechanical compaction and grouting and help define the depth and effectiveness of dynamic compaction.

4. Lateral stresses consistent with passive failure conditions were found in slicken-sided expansive clays and in a soft lake clay adjacent to a failing highway embankment. In the latter, construction was halted to prevent general bearing capacity failure. Measurement of passive stresses in toeslopes may help predict slope failures and lead to a timely application of remedial measures before slipping occurs.

5. The  $K_o$  stepped blade was used to measure lateral soil stress adjacent to existing structures including retaining walls and driven pile, thus helping to determine their stability.

6. The back-pressure system for reading pneumatic pressure cells of the stepped blade significantly improves its accuracy and ease of use.

## ACKNOWLEDGMENTS

These studies were sponsored by the Federal Highway Administration with C. Ealy the persevering contract man-

ager. Data in Figure 9 are used with the permission of Geo-Resource Consultants, Inc., San Francisco, courtesy of Eric Ng. Data in Figures 10 and 11 are used with permission of Woodward-Clyde Consultants, Inc., Denver, courtesy of Dick Davidson. Data in Figure 12 are used with permission of CTL-Thompson, Inc., Denver, and the tests were performed by C. Anderson. Data in Figure 13 are used with permission of Woodward-Clyde Consultants, Inc., Omaha, courtesy of Steve Saye. Data in Figure 14 are used courtesy of J.-L. Briaud and Texas A&M University. Many other companies and individuals also participated in these investigations, for which the authors extend their sincere thanks.

## REFERENCES

1. R. L. Handy, B. Remmes, S. Moldt, and A. J. Lutenecker. In Situ Stress Determination by Iowa Stepped Blade. *Journal of the Geotechnical Engineering Division*, ASCE, Vol. 108, No. GT11, 1982, pp. 1405-1422.
2. R. L. Handy and D. Eichner. *Back-Pressured Pneumatic Pressure Cell*. U.S. Pat. 4,662,213, 1987.
3. J. Dunnycliff. *Geotechnical Instrumentation for Monitoring Field Performance*. John Wiley & Sons, New York, 1988.
4. A. J. Lutenecker and D. A. Timian. *In Situ Tests With  $K_o$  Stepped Blade*. ASCE Special Technical Publication 6, 1986, pp. 730-751.
5. M. Pabst and R. L. Handy. *Soil Effective Stress Sensor and Method for Using Same*. U.S. Pat. 4,524,626, 1985.
6. R. L. Handy, J.-L. Briaud, K. C. Gan, C. L. Mings, D. W. Retz, and J.-F. Yang. *Use of the  $K_o$  Stepped Blade in Foundation Design*. Vol. 1, Final Report D-87/102. FHWA, U.S. Department of Transportation, June 1987.
7. E. W. K. Tse and R. L. Handy. A New Development of the  $K_o$  Stepped Blade. *Proc., 10th SE Asian Geotechnical Conference*, 1990, pp. 479-484.
8. L. J. Mahar and M. W. O'Neill. *Field Study of Pile Group Action*. Report RD-81/005. FHWA, U.S. Department of Transportation, 1980.
9. K. C. Gan. *Evaluation of the Stepped Blade Using the Pressuremeter*. Ph.D. dissertation, Texas A&M University, College Station, Texas, 1987.
10. R. L. Handy. The Arch in Soil Arching. *Journal of the Geotechnical Engineering Division*, ASCE, Vol. 111, No. 3, 1985, pp. 302-308.
11. P. Dunlop and J. M. Duncan. Development of Failure Around Excavated Slopes. *Journal of the Soil Mechanics and Foundations Division*, ASCE, Vol. 96, 1970, pp. 471-493.
12. *Assessment of In Situ Stress Changes, Jackson Lake Dam, Minidoka Project, Jackson, Wyoming*. Woodward-Clyde Consultants, Denver, Colo.; Bureau of Reclamation Embankment Dams Branch, Denver, Colo., Sept. 1987.
13. *Analysis of Instrumentation Data, Arthur C. Storz Expressway, Omaha, Nebraska*, Woodward-Clyde Consultants, Aug. 1989.

Publication of this paper sponsored by Committee on Soil and Rock Properties.